

Quasiparticle propagation in aluminum fins and tungsten TES dynamics in the CDMS ZIP detector

M. Pyle^{a,*}, P.L. Brink^a, B. Cabrera^a, J.P. Castle^a, P. Colling^a, C.L. Chang^a,
J. Cooley^a, T. Lipus^a, R.W. Ogburn^a, B.A. Young^b

^aDepartment of Physics, Stanford University, Stanford, CA 94305, USA

^bDepartment of Physics, Santa Clara University, Santa Clara, CA 95053, USA

Available online 27 December 2005

Abstract

With the aim of improving the rejection of surface beta contamination on the CDMS ZIP detector, we have studied the effectiveness of our phonon pulse-shape discrimination by matching a Monte Carlo calculation to data from a 350 μm long Al fin with W TESs (Transition-Edge Sensors) at both ends. From this fit, we determined the Al film diffusivity to be $D_{\text{Al}} = 0.010 \pm 0.001 \text{ m}^2/\text{s}$, the quasiparticle trapping length in the Al fin to be $l_{\text{trap}} = 180 \pm 10 \mu\text{m}$, and the Al to W TES transmission to be $f_{\text{Al/W}} = 0.002 \pm 0.001$.
© 2005 Published by Elsevier B.V.

PACS: 14.80.Ly; 95.35.+d

Keywords: Cold dark matter; Underground astrophysics

1. Introduction

To operate the CDMS detectors in a background free regime in the future, further improvements in discrimination ability are required [1]. One promising avenue is to increase the discrimination efficiency from our phonon pulse shapes. Such an improvement requires a better understanding of the detectors which is difficult to obtain directly. Consequently, the Cabrera group at Stanford University in 1997 designed and ran a two TES device to systematically study quasiparticle propagation in the CDMS ZIP aluminum fins.

2. Device

The quasiparticle study circuit shown in Fig. 1 was characterized with an ^{55}Fe X-ray source fluorescing on Si which produced uniformly distributed X-rays, primarily of $\sim 1.75 \text{ keV}$, with some 6 keV X-rays. A sweep of the equilibrium current through the TES, $I_{\text{W eq}}$, for bias

current, I_{b} , was performed but unfortunately lost. Therefore, the T_{c} was determined solely through small current measurements while varying the temperature of the mixing chamber, and the absolute value of the operating point current was determined by the difference in current between a fully saturated signal ($R_{\text{W}} = R_{\text{n}}$) and $I_{\text{W eq}}$.

3. Sensor dynamics and results

The dynamic response of the sensor to an energy input, $\delta q'_{\text{in}}(z, t, f_{\text{Al/W}}, D_{\text{Al}})$ (z is the spatial coordinate in the direction of current flow), can be adequately described by explicitly adding internal 1-D diffusion to the coupled nonlinear differential equations found in [4]

$$\frac{\partial T}{\partial t} = \frac{\delta q'_{\text{in}}}{C_{\text{el}} A} + \frac{I_{\text{W}}^2 \rho}{C_{\text{el}} A^2} - \frac{\Sigma}{C_{\text{el}}} (T^5 - T_{\text{sub}}^5) + D_{\text{W}} \frac{\partial^2 T}{\partial z^2} \quad (1)$$

$$L \frac{dI_{\text{W}}}{dt} = I_{\text{b}} R_{\text{s}} - I_{\text{W}} (R_{\text{s}} + R_{\text{p}} + R_{\text{W}}) \quad (2)$$

where $T(z, t)$ is the temperature of the electron system in the tungsten, C_{el} is the tungsten electronic specific heat, A is the cross-sectional area of the W TES, and D_{W} is the W

*Corresponding author. Tel.: +1 650 224 0446; fax: +1 650 725 6544.
E-mail address: mpyle1@stanford.edu (M. Pyle).

diffusion constant. The resistivity, $\rho(z, t)$, and the phonon/electron coupling term, ΣAT^5 , were both determined empirically [4].

One additional feature of this model is the explicit calculation of quasiparticle diffusion across the W TES. The spatial one-dimensionality of the above equation is allowed because D_{Al} is large enough and the transmission through the Al/W boundary, $f_{Al/W}$, is small enough that any event in or under the Al fin effectively produces a uniform quasiparticle flux across the interface into the W.

The integrals of the current pulses for channel A and channel B are plotted against each other in Fig. 2. The

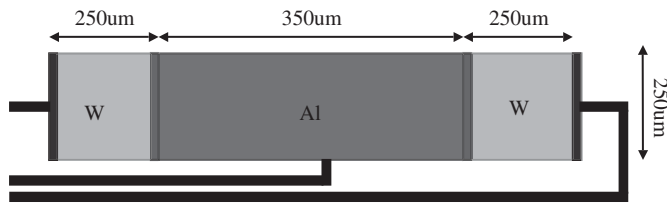


Fig. 1. Schematic of quasiparticle test circuit which was fabricated using a process similar to that used for CDMS ZIP detectors [2]. The notable exceptions are the lack of an amorphous Si layer between the Al/W and the substrate, the thickness of the Al being ~ 150 nm rather than ~ 350 nm, and the Si substrate being 1 mm thick. The Al fin also serves as the connection to ground for both TESs. Testing of this device occurred with an electronic setup similar to that used by Stanford X-ray detector research [3].

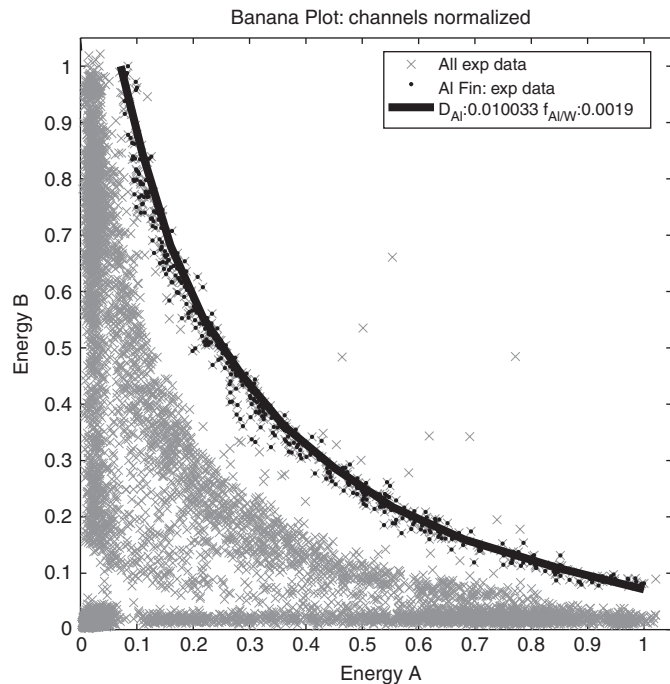


Fig. 2. Scatter plot of E_A vs. E_B : Since the shunt resistor, R_s , is $< R_W$, the device is effectively voltage biased, and as such, the energy input to the device is to a high degree of accuracy independent of the pulse shape and linear with respect to the $\int \Delta I_W dt$ as long as the transition width $\ll T_c$. Both channels were normalized to the maximum energy seen in the Al banana shape.

primary region of interest is the curved banana-shaped region in which energy is shared between the two TESs. We interpret these events as occurring within the Al fin. If no quasiparticle trapping mechanism existed within the Al, then this curved region would be a diagonal straight line. Following Refs. [5,6], the attenuation length, $l_{\text{trap}} = \sqrt{D_{Al}\tau_{\text{trap}}}$, was confirmed to be $180 \pm 10 \mu\text{m}$.

The dearth of events below this banana region illustrates that events which interact in the Si substrate, even directly beneath the central Al fin, have a lower efficiency for energy absorption into the TES, as expected from phonon escape.

The banana is also separated from axis events, indicating that the Al to W transmission $f_{Al/W}$ is small. We used a 1-D diffusive Monte Carlo coupled to a TES simulator that solved Eqs. (1) and (2), which were developed as part of a larger CDMS ZIP Monte Carlo, to match the experimental Al pulses. Degeneracy between D_{Al} , $f_{Al/W}$, and l_{trap} required that the time delay between the start of the two channels be fit concurrently (see Fig. 3).

Pulses from both channels for an event near the center of the Al fin are shown in Fig. 4. These pulses are representative of all pulses from events that occurred in the Al as well as events that hit the substrate beneath the Al. They display two very different fall times. By contrast, the relative size of the initial spike varies drastically for events occurring directly in the W and in $\sim 30\%$ of these events the spike is totally absent. Consequently, the spike must be physical and cannot simply be caused by downstream electronics. One possible production mechanism is the relatively slow quasiparticle diffusion across the W. To see this, note that if the TES is biased on the transition in a region where $\partial^2 \rho / \partial E^2 > 0$ (i.e below T_c) then concentrating the energy within one portion of the TES increases ΔR

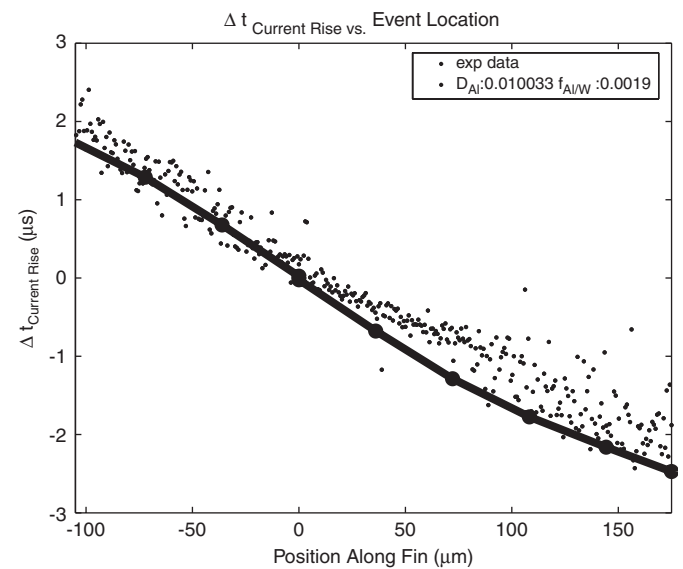


Fig. 3. Time delay between the start of the pulses for channels A and B as a function of position along the Al fin. The simulated line corresponds to $D_{Al} = 0.01 \text{ m}^2/\text{s}$. The position of events was determined by correlating the location along the banana with location along the fin.

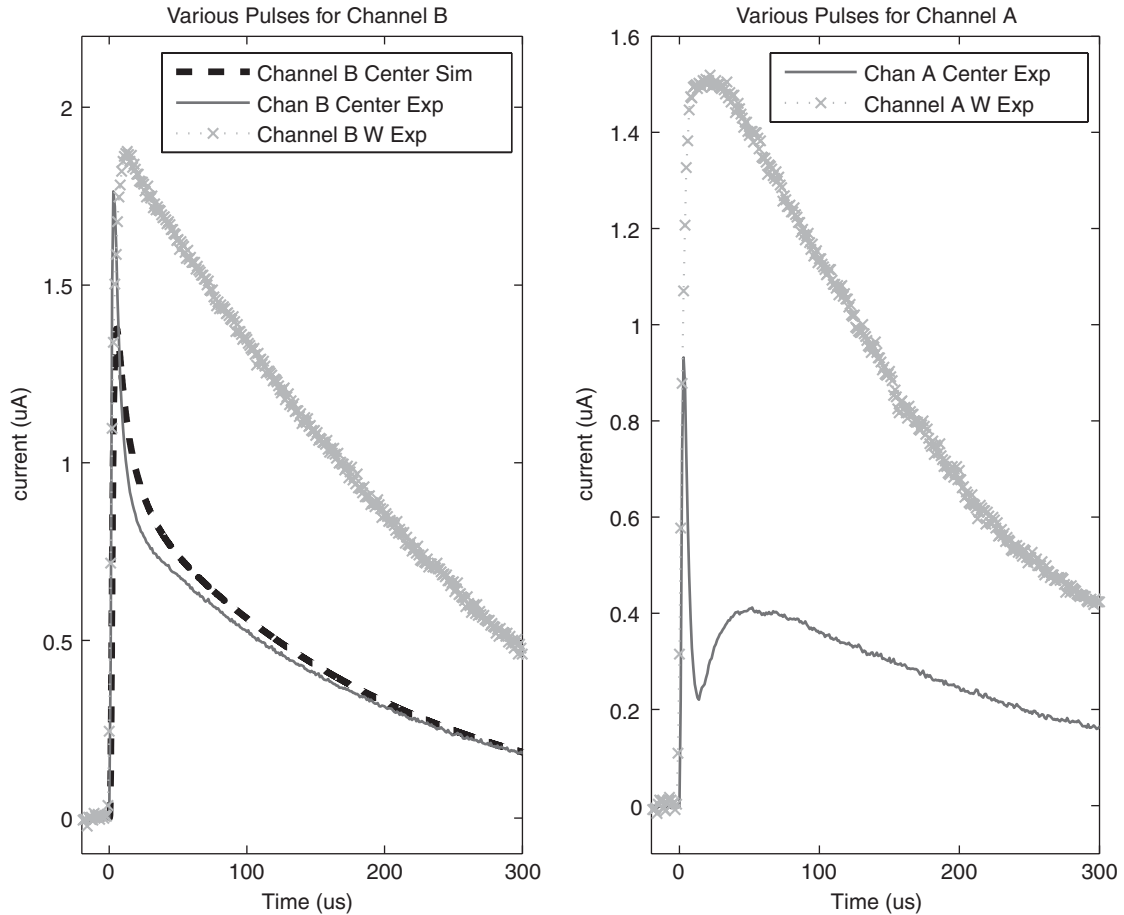


Fig. 4. Pulses for each channel from an event near the center of the Al fin (lower traces), and events occurring directly in the TESs (upper traces). A simulated pulse is shown for channel B.

more than distributing the energy evenly as long as this portion is chosen such that it is in series with the rest of the device. Simulations of this mechanism (Fig. 4) qualitatively and almost quantitatively agree with the experiment for channel B if D_W is simulated as $< 0.0003 \text{ m}^2/\text{s}$. This is $\sim \frac{1}{5}$ of the simplistic D_W calculated from ρ_W . Lowering the bias current in the simulation increases the simulation's ability to reproduce the experiment as well as increasing best fit D_W .

The overall normalization difference of 22% between the two channels and the dip seen in channel A's pulse shape are surprising and may require additional physics or a loosening of experimental assumptions (systematic error in bias voltage, non-uniform T_c across the TES) for explanation.

4. Conclusions

A greater understanding of the quasiparticle propagation in the Al fins, the transfer characteristics of Al/W interface, and the relevant diffusion coefficients are all vital pieces to an overarching detector Monte Carlo for the

CDMS ZIP detector. The next analysis step will be to study the interface between the Ge (or Si) substrate and the Al film and to understand the two asymmetries seen between the two devices.

Acknowledgements

This work is supported by the Department of Energy contracts DE-FG03-90ER40569 and DE-FG02-04ER41295-A002. The samples were fabricated in the Stanford Nanofabrication Facility, sponsored by NSF under Grant ECS-0335765.

References

- [1] P.L. Brink, et al., these proceedings.
- [2] D.S. Akerib, CDMS, et al., Phys. Rev. D 68 (2003) 82002.
- [3] S.W. Leman, these proceedings.
- [4] B. Cabrera, Nucl. Instr. and Meth. A 444 (2000) 304.
- [5] H. Kraus, et al., Phys. Lett. B 231 (1989) 195.
- [6] T. Saab, et al., Nucl. Instr. and Meth. A 444 (2000) 300.